Journal of Alloys and Compounds 500 (2010) 108–112

Contents lists available at ScienceDirect

Journal of Alloys and Compounds

journal homepage: www.elsevier.com/locate/jallcom

Synthesis of Sr_2SiO_4 nanometer particles from the core–shell precursor of $SrCO_3/SiO_2$

Yu-Lun Chang, Hsing-I Hsiang*, Fa-Tai Lan, Li-Then Mei, Fu-Su Yen

Particulate Materials Research Center, Department of Resources Engineering, National Cheng Kung University, No. 1, University Road, 70101 Tainan, Taiwan, ROC

ARTICLE INFO

Article history:
Received 30 July 2009
Received in revised form 25 March 2010
Accepted 1 April 2010
Available online 8 April 2010

Keywords:
Sr_2SiO_4
Core–shell
Solid-state reaction

ABSTRACT

This study presents the formation mechanism for Sr_2SiO_4 synthesized from coated $SrCO_3$ with gel-derived SiO_2. The experimental results indicate that Sr_2SiO_4 formation from the mechanical mixed precursor with poor mixing homogeneity was dominated by the thermal decomposition of $SrCO_3$ at higher temperatures. Conversely, the $SrCO_3/SiO_2$ core–shell precursor can facilitate the formation of Sr_2SiO_4 from the direct reaction between $SrCO_3$ and SiO_2 at lower calcination temperatures. In addition, raising the coating pH and temperature can promote the shell layer growth that further facilitated Sr_2SiO_4 formation. A nearly pure α-Sr_2SiO_4 product with particle size around 20–50 nm can be obtained at 800 °C for 3 h.

1. Introduction

Strontium silicate, Sr_2SiO_4, is a potential host material for luminescent appliances. It has two crystalline phases, monoclinic (β) and orthorhombic (α), with a transformation temperature of about 85 °C. Their crystal structures are the same as those of β-Ca_2SiO_4 and β-K_2SO_4, respectively [1]. Orthorhombic Sr_2SiO_4: Eu^{2+} is an important yellow phosphor candidate that can be used to develop white light-emitting diodes (LEDs) in combination with a GaN chip [2]. Various activators and co-activators were added to develop the afterglow luminescence of Sr_2SiO_4 phosphors [3,4]. Sr_2SiO_4 powders can be prepared using many techniques, such as solid-state reaction [3,4], sol–gel method [5], precipitate method [6], and spray pyrolysis [7]. Because of its inexpensive cost and convenient production process, Sr_2SiO_4 powders are conventionally synthesized using the solid-state reaction.

Sr_2SiO_4 powder is usually prepared using a solid-state reaction between $SrCO_3$ and SiO_2 at a temperature above 1200 °C [3,4]. High-temperature calcination easily leads to coarsening and agglomeration of the resulting particles. Recently, Buscaglia et al. [8] used a novel core–shell technique by coating $BaCO_3$ with TiO_2 to improve the mixing extent of the reactants and reported that the core–shell structure can increase the contact area between $BaCO_3$ and TiO_2, facilitating the formation of $BaTiO_3$ at lower temperatures. The inorganic particle coating technique using different compounds was studied extensively. A common example is to use metal alkoxides hydrolysis and condensation reactions to form metal oxide shells on the surfaces of core inorganic particles. The silica coating via the sol–gel route from TEOS is an effective tool to engineer the inorganic particle surface and has been used in many applications [9–11].

In this study, $SrCO_3$ coated with gel-derived SiO_2 was used as the precursor to synthesize Sr_2SiO_4 powders. The SiO_2 shell coated onto the $SrCO_3$ surface was formed using TEOS hydrolysis and condensation reactions. The SiO_2 coating on the $SrCO_3$ surface was confirmed using TEM (transmission electron microscopy), FT-IR (Fourier transformation infrared spectroscopy), and zeta potential measurements. The Sr_2SiO_4 solid-state reaction mechanism was investigated using X-ray diffractometry (XRD) and differential thermogravimetry and thermgravimetry (DTA/TG).

2. Experimental

In order to fulfill the nano-scale coating, the $SrCO_3$ (Aldrich, 99.99%) was premilled using 5 and 3 mm zirconia balls for 48 and 24 h, respectively. The obtained $SrCO_3$ particles had sizes around 160 nm. The pre-treated $SrCO_3$ particles were then dispersed into an aqueous solution at pH = 8. On the other hand, TEOS (Jassen Chimica, 98%) was hydrolyzed in the EtOH with HNO_3 (aq) at pH = 4. Then, the hydrolyzed sol was dropped into the $SrCO_3$ slurry under magnetic stirring for 36 h at pH = 6.7. The resulted core–shell mixtures were further dried using vacuum evaporation. The reference mixture is prepared using mechanical mixing of pre-treated $SrCO_3$ particles and dried SiO_2 gel which is derived from TEOS. The mixtures were then calcined at different temperatures in air.

The crystalline phase identification was determined using X-ray diffractometry (Siemens, D5000) with Cu-K_α radiation. Electrophoretic measurements of the starting materials under different pH values were performed on a zeta potentiometer (Malvern, Zetasizer, Nano ZS). The TEM (Jeol, JEM-3010) was used to observe the crystallite size and morphology. Semi-quantitative determination of the element content was detected using EDS (Noran, Voyager 1000) attached to the TEM. The DTA/TG analysis was performed using a thermal analysis instrument (Netzsch STA, 409 PC) under 40 ml/min air flow rate.

---

* Corresponding author. Tel.: +886 6 2757575x62821; fax: +886 6 2380421.
E-mail address: hsingi@mail.ncku.edu.tw (H.-I. Hsiang).

0925-8388/$ – see front matter © 2010 Elsevier B.V. All rights reserved.
doi:10.1016/j.jallcom.2010.04.002

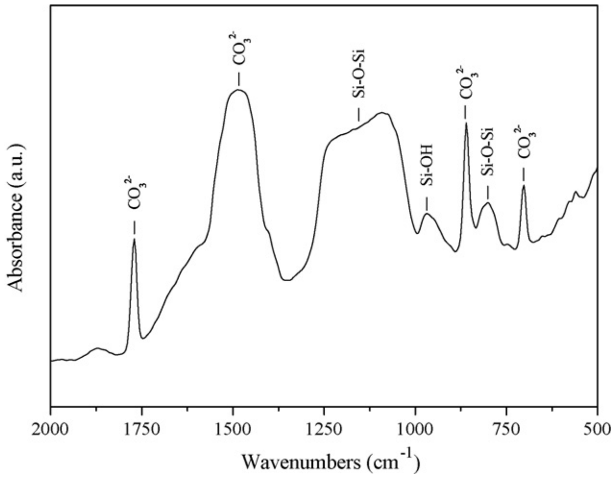

Fig. 1. The FT-IR spectrum of the $SrCO_3/SiO_2$ core–shell precursor.

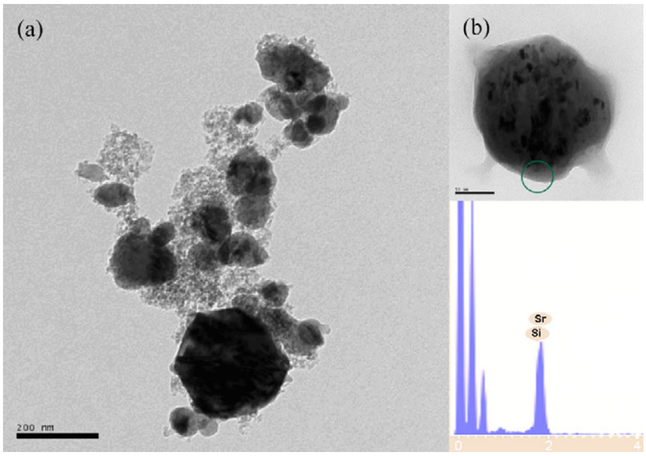

Fig. 2. TEM photographs of the $SrCO_3/SiO_2$ core–shell precursor.

3. Results and discussion

Fig. 1 shows FT-IR spectrum of the $SrCO_3/SiO_2$ core–shell precursor. The absorption peaks at 1768, 1450, 1070, 860, 706 and 699 cm^{-1} are assigned to $SrCO_3$ stretching characteristics [12]. Si–O–Si (800 cm^{-1} [13] and 1000–1200 cm^{-1} [14]) and Si–OH (970 cm^{-1} [15]) were also observed, indicating the formation of SiO_2 with a small amount of silanol groups. Fig. 2(a) shows TEM photograph of the $SrCO_3/SiO_2$ core–shell precursor. The dark particles with a larger size of 100–200 nm are the $SrCO_3$ raw material. The tiny particles with a size of about 10 nm are identified as the gel-derived SiO_2. It is observed that the gel-derived SiO_2 particles locate onto the $SrCO_3$ surfaces and also agglomerate at the particle junctions. In addition, an amorphous layer was also observed on the $SrCO_3$ surface (Fig. 2(b)). According to the EDS analysis, both Sr-element and Si-element were identified, indicating the coating of SiO_2 layer onto the $SrCO_3$ surfaces. From the electrophoretic measurement (Fig. 3), the $SrCO_3/SiO_2$ core–shell precursor shows a negative surface charge as same as pure SiO_2. This result confirms that the gel-derived SiO_2 shell was formed on the surfaces of the $SrCO_3$ powders.

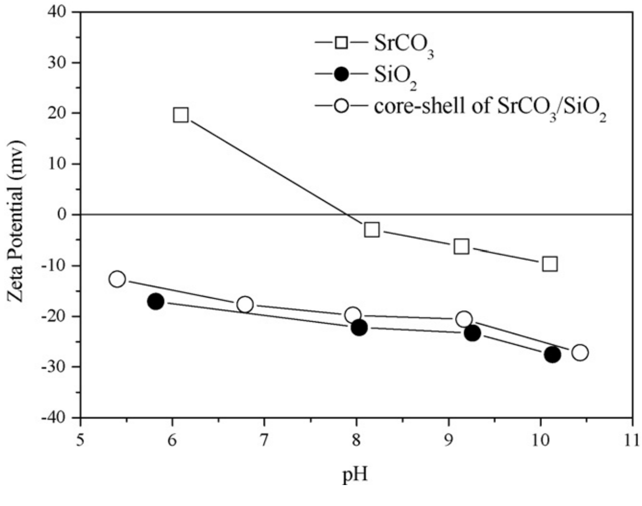

Fig. 3. Zeta potential for the $SrCO_3/SiO_2$ core–shell precursor.

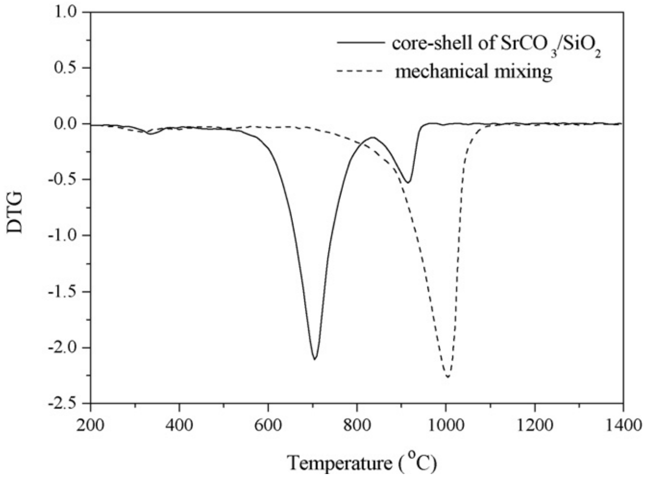

Fig. 4. DTG curves of the core–shell and mechanical mixing precursors.

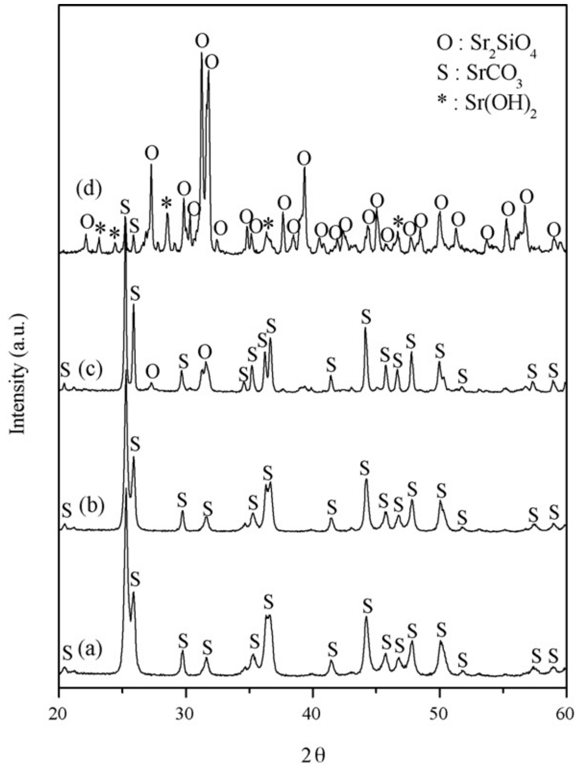

Fig. 5. XRD patterns of the mechanical mixing precursors calcined at different temperatures for 1 h, (a) without calcination, (b) 600 °C, (c) 800 °C, and (d) 1100 °C.

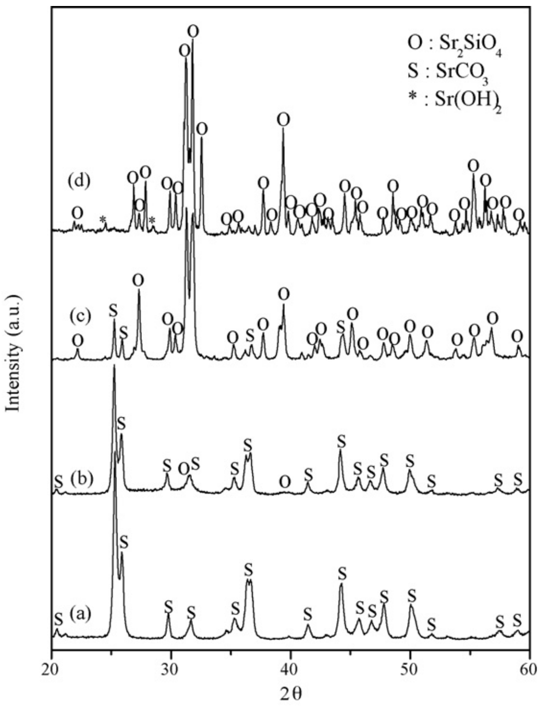

Fig. 6. XRD patterns of the core–shell precursor calcined at different temperatures for 1 h, (a) without calcination, (b) 600 °C, (c) 800 °C, and (d) 1100 °C.

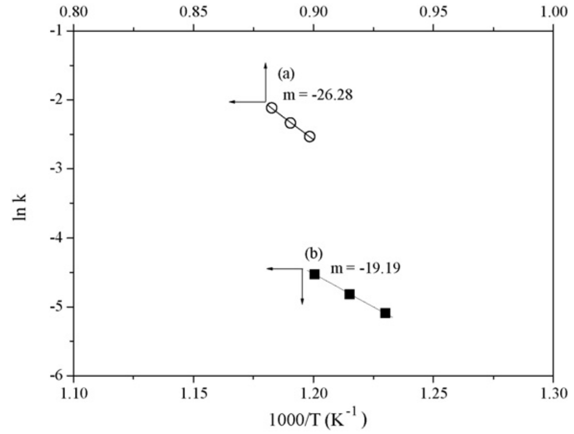

Fig. 7. Arrhenius plots for different reaction temperature regions, (a) 540–560 °C, and (b) 840–860 °C.

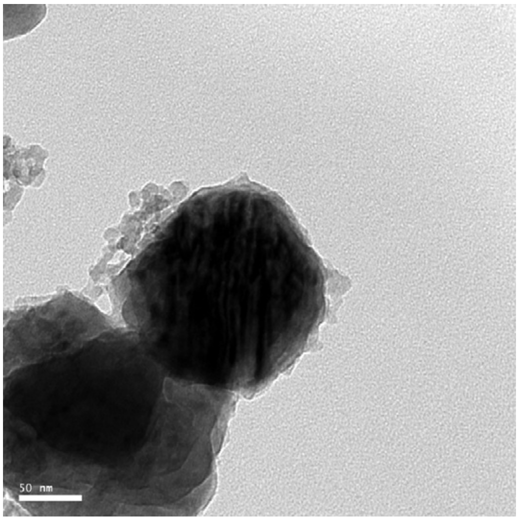

Fig. 8. TEM photographs of the core–shell precursor at pH = 8 and 50 °C.

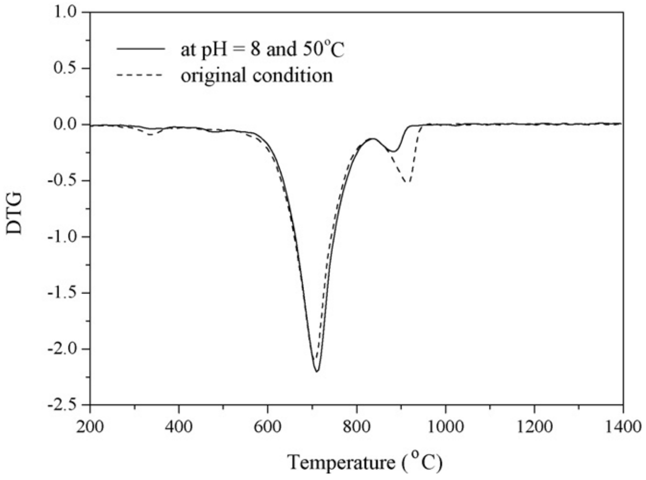

Fig. 9. DTG curves of the core–shell precursor with original condition and at pH = 8 and 50 °C.

Fig. 4 shows DTG curves of the core–shell precursor and the precursor prepared using mechanical mixing. It indicates that the precursor prepared using mechanical mixing has only one weight loss stage starting at around 700 °C. Nevertheless, the core–shell precursor shows two stages of weight loss, i.e. the first stage starting at around 500 °C, and another at near 800 °C. An overlapping of the second weight loss stage in the core–shell precursor and the weight loss of the precursor prepared using mechanical mixing was observed. Figs. 5 and 6 show XRD patterns of the precursors prepared using mechanical mixing and the core–shell precursors calcined at different temperatures, respectively. For the precursor prepared using mechanical mixing, the formation of Sr_2SiO_4

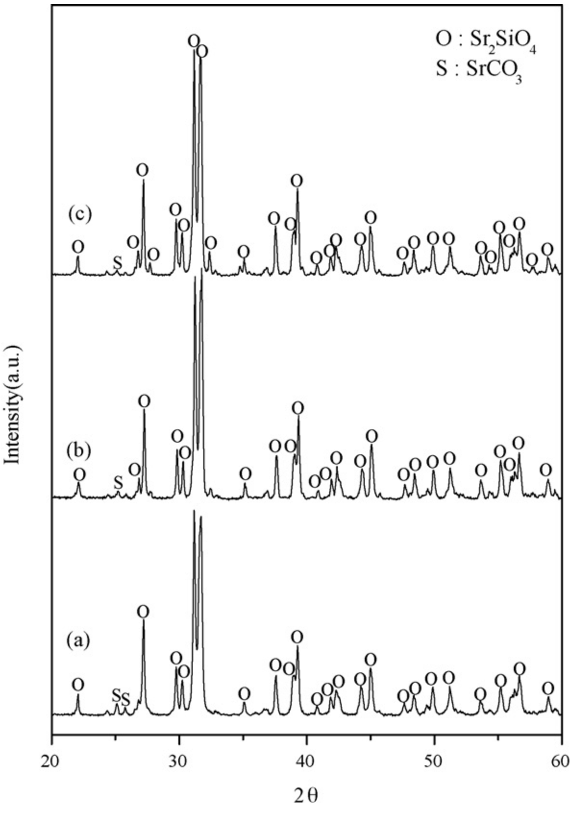

Fig. 10. XRD patterns of the core–shell precursor at pH = 8 and 50 °C calcined at 800 °C for different periods of time, (a) 1 h, (b) 2 h, and (c) 3 h.

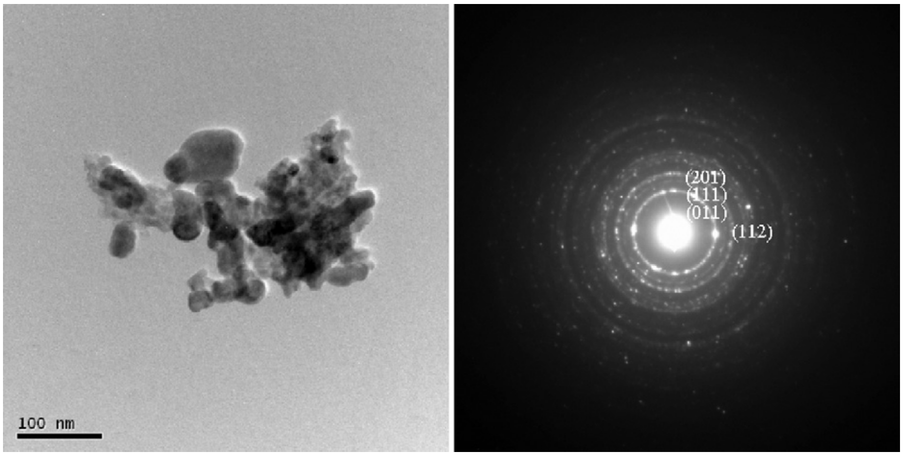

Fig. 11. TEM photographs of the core–shell precursor at pH = 8 and 50 °C calcined at 800 °C for 3 h.

(α) was observed at 800 °C. At 1100 °C, the amount of the Sr_2SiO_4 (α + β) formation increased drastically and a small amount of $SrCO_3$ was still remained. On the other hand, the core–shell precursor reveals the formation of Sr_2SiO_4 (α) at 600 °C. When the temperature was raised to 800 °C, a great amount of Sr_2SiO_4 (α) was formed. At 1100 °C, a nearly pure Sr_2SiO_4 (α + β) was obtained. It is obvious that Sr_2SiO_4 formation was facilitated drastically for the core–shell precursor. Besides, a trace amount of strontium hydroxides was observed. It is probably due to hydration of unreacted SrO with the moisture in air.

Yamaguchi et al. reported that the formation of Sr_2SiO_4 occurs preferably for mixtures with any ratio of $SrCO_3$ and SiO_2 in the heat treatment [16]. In this study, for the core–shell precursor, the formation of Sr_2SiO_4 can be formed at a temperature as low as 600 °C. The activation energy for the first stage reaction of the core–shell precursor is about 159 kJ/mol (Fig. 7), which is also similar to the reported value for the formation of Sr_2SiO_4 [17]. Therefore, the first reaction stage of the core–shell precursor can be ascribed to the direct reaction between $SrCO_3$ and SiO_2 to form Sr_2SiO_4 (Eq. (1)). Moreover, the activation energy for the second stage reaction of the core–shell precursor is about 210 kJ/mol (Fig. 7). It just coincides with the activation energy of the thermal decomposition of $SrCO_3$ [18], indicating $SrCO_3$ decomposing thermally itself (Eq. (2)). Then the resulted SrO diffuses rapidly through the product layer to carry on the Sr_2SiO_4 formation (Eq. (3)). Conversely, the precursor prepared using mechanical mixing provides poor mixing homogeneity of the reactants that the direct reaction between $SrCO_3$ and SiO_2 to form Sr_2SiO_4 occurs unfavorably [19]. Therefore, the reaction mechanism for the mechanically mixing precursor mainly takes place via the reactions (Eq. (2)) and (Eq. (3)) at a higher temperature.

$$2SrCO_3 + SiO_2 \rightarrow Sr_2SiO_4 + 2CO_2 \quad (1)$$

$$SrCO_3 \rightarrow SrO + CO_2 \quad (2)$$

$$2SrO + SiO_2 \rightarrow Sr_2SiO_4 \quad (3)$$

To prevent the formation of agglomerated SiO_2 particles and promote the growth of the SiO_2 layer of the core–shell precursor, pH value and coating temperature were both raised. It is expected to enhance the dissolution and precipitation of SiO_2 that causes Ostwald ripening from particles to coated layers. When the coating condition was at pH = 8 and 50 °C, the TEM photograph indicates that the amorphous SiO_2 layer coated on the $SrCO_3$ surface becomes thicker and the agglomeration of SiO_2 particles almost diminishes (Fig. 8). Fig. 9 shows DTG curve of the resulting core–shell precursor prepared at pH = 8 and 50 °C. It shows that the second stage reaction is suppressed significantly. The reaction mechanism almost takes place via the lower temperature reaction, i.e. Eq. (1). Fig. 10 shows XRD patterns of the core–shell precursor calcined at 800 °C for different periods of time. Compared with Fig. 6, it is seen that the increment of coating pH value and temperature for the core–shell precursor can accelerate the Sr_2SiO_4 formation, and reduce the amount of remaining $SrCO_3$. By increasing the holding time to 3 h, a nearly pure α-Sr_2SiO_4 product with particle size around 20–50 nm can be obtained (Fig. 11).

4. Conclusions

In this study, the solid-state reaction between $SrCO_3$ and SiO_2 can be separated into two stages, i.e. the direct reaction from $SrCO_3$ and SiO_2 to form Sr_2SiO_4, and the reaction involving the thermal decomposition of $SrCO_3$ itself. The experimental results indicate that Sr_2SiO_4 formation from the mechanical mixed precursor with poor mixing homogeneity was dominated by the thermal decomposition of $SrCO_3$ at higher temperatures. Conversely, the $SrCO_3/SiO_2$ core–shell precursor can facilitate the formation of Sr_2SiO_4 from the direct reaction between $SrCO_3$ and SiO_2 at lower calcination temperatures. The increment of coating pH and temperature can further enhance SiO_2 shell layer growth onto the $SrCO_3$ particle surface and prevent the formation of agglomerated SiO_2 particles. Therefore, the formation rate of Sr_2SiO_4 was further facilitated, and a nearly pure α-Sr_2SiO_4 product with particle size around 20–50 nm can be obtained at 800 °C for 3 h.

Acknowledgments

The work was financially co-sponsored by the Ministry of Economic Affairs of the Republic of China through contract (97-EC-17-A-08-S1-023) and National Science Council of the Republic of China (NSC 97-2221-E-006-010).

References

[1] S.H.M. Poort, W. Janssen, G. Blasse, J. Alloys Compd. 260 (1997) 93.
[2] J.K. Park, M.A. Lim, C.H. Kim, H.D. Park, J.T. Park, S.Y. Choi, Appl. Phys. Lett. 82 (2003) 683.
[3] L. Zhang, X. Zhou, H. Zeng, H. Chen, X. Dong, Mater. Lett. 62 (2008) 2539.
[4] N. Lakshminarasimhan, U.V. Varadaraju, Mater. Res. Bull. 43 (2008) 2946.
[5] W.H. Hsu, M.H. Sheng, M.S. Tsai, J. Alloys Compd. 467 (2009) 491.
[6] I. Netteship, J.L. Shull, W.M. Kriven, J. Eur. Ceram. Soc. 11 (1993) 291–298.
[7] H.S. Kang, S.K. Hong, Y.C. Kang, K.Y. Jung, Y.G. Shul, S.B. Park, J. Alloys Compd. 402 (2009) 246.
[8] M.T. Buscaglia, V. Buscaglia, R. Alessio, Chem. Mater. 19 (2007) 711.
[9] L.M.L. Marzan, M. Giersig, P. Mulvaney, Langmuir 12 (1996) 4329.
[10] M. Ohmori, E. Matuevic, J. Colloid Interface Sci. 160 (1993) 288.

[11] R.A. Caruso, M. Antonietti, Chem. Mater. 13 (2001) 3272.
[12] C. Zhang, W. Jiang, X. Yang, Q. Han, X. Wang, J. Alloys Compd. 474 (2009) 287.
[13] D.L. Ou, A.B. Seddon, J. Non Cryst. Solids 210 (1997) 187.
[14] Y.L. Lin, T.J. Wang, Y. Jin, Powder Technol. 123 (2002) 194.
[15] E. Liden, L. Bergstrom, M. Persson, R. Carlsson, J. Eur. Ceram. Soc. 7 (1991) 361.
[16] O. Yamaguchi, K. Yabuno, K. Takeoka, K. Shimizu, Chem. Lett. 5 (1979) 401.
[17] C.H. Lu, P.C. Wu, J. Alloys Compd. 466 (2008) 457.
[18] B.V. Lvov, V.L. Ugolkov, Thermochim. Acta 410 (2004) 47.
[19] V.V. Gusarov, Russ. J. Gen. Chem. 67 (1997) 1846.